MATHEMATICAL MODELLING OF FLOOD WAVE: A CASE STUDY OF BUDALANG'I FLOOD PLAIN BASIN IN BUSIA COUNTY, KENYA

BY

Stephen Musindayi Miheso

A THESIS SUBMITTED IN PARTIAL FULFILMENT OF THE REQUIREMENTS FOR THE DEGREE OF MASTER OF SCIENCE IN APPLIED MATHEMATICS

SCHOOL OF MATHEMATICS, STATISTICS AND ACTUARIAL SCIENCE

MASENO UNIVERSITY

© 2022.

DEDICATION

To my father, Evans Alusiola and my Mother Beatrice Nekesa for their constant
encouragement
and support for me to complete this thesis. I also dedicate this thesis to my dear
wife Leah Amisi and daughter
Beatrice Musindayi for their consistent support morally, spiritually and
financially.

Abstract

Flooding is a worldwide problem with more adverse effects in developing countries. In Kenya, severe flooding is experienced on the lower tributaries of Lake Victoria, mainly Budalang'i area. This is indicated in the historical floods of 2003, 2007, 2017 and 2019, leading to mass displacement of people and property destruction. This has attracted attention of researchers worldwide and application of different measures to curb flood in the study regions. Mathematical modeling of flood wave has however not been adopted in Budalang'i flood plain. Therefore this study formulated, analyzed and simulated the $2D$ flood wave model with incorporation of a sink to the Budalangi flood plain. Formulation was applied on existing Navier Stokes equations with the addition of a sink term on continuity equation. Analysis of the shallow water model entailed transforming the equations using Jacobian transformation and assessing the nature of flow using Froude number. For simulations of the $2D$ shallow water model, the study adopted a finite difference scheme to make approximations which solved the system of equations and displayed in the figures . It is realized that in the formulation of the $2D$ shallow equations, appropriate model for Budalang'i flood plain is easily derived from the $3D$ Navier Stokes equations under flood plain assumptions and addition of a sink term is necessary for modelling in the flood plain. Assessment of the properties reveals that supercritical flows are dominant. Addition of a sink term ensures steady state velocity thus reducing higher frequency and turbulence as well as over bank flows while incorporating coriolis term has significant effect on the turbulence. The study concludes that addition of a sink term to the $2D$ shallow water model will enable control of the floods in the area of study. The findings will aide disaster management stakeholder to come up with a more reliable flood prevention technique and new knowledge on how source terms can help reduce flood risk.

Contents

Index of Notations

Chapter 1

Introduction

This chapter contains the background of the study, basic concepts, statement of the problem, objectives of the study, methodology and significance of the study. These are presented in the subsequent sections

1.1   Background of the Study

A flood is a large amount of water moving along the earth's surface in an uncontrolled manner [21]. Mathematical modelling of flood propagation is therefore the quantitative description of the characteristics and evolution of this flow that is set up. The quantitative description includes the external boundaries and internal geometry of the system, the boundary conditions, and the flow terms are considered. The main aim of mathematical modelling of $2D$ is the development of a mathematical framework that entail algorithms to numerically approximate flow behaviour in an area. [10] Floods in a given area mainly originate from long term rains or failure of a dam or some other water control structure. Floods can be slow, extreme or violent based on the nature of their origin. Mathematical modelling of floods dates back to the 1960's at the time the first models were suggested

Ponce[40]. However, over the past decades, many flood prediction models have been developed and reported in the literature[5]. Flood modelling is governed by laws that indicate the physical changes that take place in the flow processes [35]. The fundamental mathematical laws that govern the flood phenomenon are the Navier-Stokes equations. Their solutions are however practically impossible for the space and time scales of any real case leading to the need of simplified descriptions such as the shallow water equation (SWE) model which is now widely used [10]. Over time, the development of the shallow water model has been widely used to model different physical phenomena of water flows such as flood waves, dambreaks, tidal flows in estuary, coastal water regions and bore wave propagation in rivers among other uses. Substantial effort has been devoted to the development of computational techniques for that kind of fluid flow simulations [15]. However, most of the studies carried out have dwelt on $1D$ models and for those that have attempted the $2D$ model, they have failed to include a sink term which is very significant in modelling. The purpose of this study was to carry out flood propagation by means of modelling the $2D$ shallow water system of equations with application to the Budalangi flood plain in Busia County, Kenya.

1.2 Basic Concepts

1.2.1 Free Surface

This is the surface of a fluid that is subject to zero parallel shear stress, such as the interface between two homogeneous fluids, for example, liquid water and the air in the earth's atmosphere. Unlike liquids, gases cannot form a free surface on their own. Fluidized/liquified solids, including slurries, granular materials and powders

may form a free surface.

1.2.2   Navier Stokes Equations

These are equations that describe the motion of viscous fluid substances. These equations are in the balance form and arise from applying Isaac Newton's second law to fluid motion. The assumption that the stress in the fluid is the sum of a diffusing viscous term (proportional to the gradient of velocity) and a pressure term hence describing viscous flow is added. The main difference between them and the simpler Euler equations for inviscid flow is that Navier Stokes equations also factor in the Froude limit (no external field) and are not conservation equations, but rather a dissipative system, in the sense that they cannot be put into the quasilinear. They are expressed as follows,

$$\left(\frac{\partial u}{\partial x} + \frac{\partial v}{\partial y} + \frac{\partial w}{\partial z} \right) = 0$$

$$\rho \left(\frac{\partial u}{\partial t} + u\frac{\partial u}{\partial x} + v\frac{\partial u}{\partial y} + w\frac{\partial u}{\partial z} \right) = F_x - \frac{\partial p}{\partial x} + \left(\frac{\partial \tau_{xx}}{\partial x} + \frac{\partial \tau_{xy}}{\partial y} + \frac{\partial \tau_{zx}}{\partial z} \right)$$

$$\rho \left(\frac{\partial v}{\partial t} + u\frac{\partial v}{\partial x} + v\frac{\partial v}{\partial y} + w\frac{\partial v}{\partial z} \right) = F_y - \frac{\partial p}{\partial y} + \left(\frac{\partial \tau_{xy}}{\partial x} + \frac{\partial \tau_{yy}}{\partial y} + \frac{\partial \tau_{zy}}{\partial z} \right) \tag{1.1}$$

$$\rho \left(\frac{\partial w}{\partial t} + u\frac{\partial w}{\partial x} + v\frac{\partial w}{\partial y} + w\frac{\partial w}{\partial z} \right) = F_z - \frac{\partial p}{\partial z} + \left(\frac{\partial \tau_{xz}}{\partial x} + \frac{\partial \tau_{yz}}{\partial y} + \frac{\partial \tau_{zz}}{\partial z} \right).$$

where the first equation is the mass conservation equation in the three dimensions, which are x, y, z. ρ in the next three momentum equations represents the fluid density. $F_{x,y,z}$ terms represent force in the respective directions (that is, the directional momentum). The partial derivatives $\frac{\partial p}{\partial x}$, $\frac{\partial p}{\partial y}$ and $\frac{\partial p}{\partial z}$ represents the change in pressure in the x, y and z directions. τ indicates the viscous shear stresses due to the fluid change in momentum.

1.2.3 Catchment

A surface water catchment is the total area that drains into a river. A groundwater catchment is the total area that contributes to the groundwater component of the river/basin flow.

1.2.4 Flood Plain

Refers to any area of land over which water flows or is stored during a flood event or would flow but for the presence of flood defences.

1.2.5 Hydraulic Model

A simplified physical representation of a scaled flow within a river system. It can be sketched in different dimensions and thus we may not have a specific general model. In fluid dynamics, it represents a sketch that can picture and visualize flow field before coming up with a specific design. It is used within the catchment flood management plan to test the influence of flood risk management measures on flooding.

1.2.6 The Shallow Water Model

The shallow water model was formulated from the Navier Stokes equations under the assumption of larger horizontal scale compared to vertical scale. Below is a typical shallow water model.

$$\frac{\partial U}{\partial t} + \frac{\partial F(U)}{\partial x} + \frac{\partial G(U)}{\partial y} = S(U) \tag{1.2}$$

where

$$U = \begin{bmatrix} h \\ hu \\ hv \end{bmatrix}, \quad F(U) = \begin{bmatrix} hu \\ hu^2 + \frac{1}{2}gh^2 \\ huv \end{bmatrix}, \quad G(U) = \begin{bmatrix} hv \\ huv \\ hv^2 + \frac{1}{2}gh^2 \end{bmatrix}, \quad \text{and}$$

$$S(U) = \begin{bmatrix} 0 \\ gh(S_{ox} - S_{fx}) \\ gh(S_{oy} - S_{fy}) \end{bmatrix},$$

from which, u and v denote the velocity components in the x and y directions respectively, h indicates the water depth, g is the acceleration due to gravity, b is the bottom elevation, S_{fx} and S_{fy} are the frictions in the x and y directions respectively, whereby

$$S_{fx} = \frac{n^2 u \sqrt{u^2 + v^2}}{h^{\frac{4}{3}}}$$

and

$$S_{fy} = \frac{n^2 v \sqrt{u^2 + v^2}}{h^{\frac{4}{3}}}$$

in which n denotes Mannings Roughness Coefficient. Thus the full system of shallow water equations can be written in conservation form as,

$$\frac{\partial h}{\partial t} + \frac{\partial hu}{\partial x} + \frac{\partial hv}{\partial y} = 0$$

$$\frac{\partial hu}{\partial t} + \frac{\partial (hu^2 + \frac{1}{2}gh^2)}{\partial x} + \frac{\partial huv}{\partial y} = -gh\frac{\partial b}{\partial x}$$

$$\frac{\partial hv}{\partial t} + \frac{\partial huv}{\partial x} + \frac{\partial (hv^2 + \frac{1}{2}gh^2)}{\partial y} = -gh\frac{\partial b}{\partial y}$$

where u and v are the horizontal and vertical velocities respectively, b represents the change in bed slope source term and friction source term S_f in the x or y directions. The other variables, g represents force of gravity, h represents water height and t represents time. On the right hand side, the change in bed slope source

terms are negative implying that the bottom is a material surface of the fluid and therefore not crossed by the flow. Under some assumption and successful derivation of appropriate model for the flood plain, a Froude number can be obtained.

1.3   Statement of the Problem

Budalang'i flood plain basin has been experiencing consistent floods on the onset of heavy rains causing loss of lives, destruction of property, outbreak of water borne diseases and siltation of arable lands. In the recent past, the frequency and intensity of the floods has greatly increased, partially attributed to climate change and human activities in the area. In response, few methods have been proposed to solve the flood occurrences with little success. Mathematical approach to the solution of the problem using advanced technology such as inundation analysis of floods using computer-based models and flood routing, has however not been fully adopted in the area of study. The few mathematical approaches developed have also not adopted flood wave modeling as an approach to model the phenomena. This study therefore sought to formulate and analyze the $2D$ flood wave model incorporating coriolis force and sinks for Budalang'i flood plain.

1.4   Objectives of the study

The general objective of the study was to carry out mathematical modelling of flood wave in Budalang'i flood plain in Busia County, Kenya.
The specific objectives of the study were to:

1. Formulate a $2D$ mathematical flood wave model for Budalang'i flood plain basin.

2. Analyze the $2D$ mathematical flood wave model for Budalang'i flood plain basin.

3. Carry out the $2D$ mathematical flood wave model simulations for Budalang'i flood plain basin.

1.5   Methodology

In objective one, the study sought to formulate the $2D$ shallow water model appropriate for Budalang'i flood plain. Formulation followed from the reduction of the $3D$ Navier Stokes equations using Leibnitz and Chain Rules. Each of the terms of the system of equations were integrated respectively, factored and terms recollected in the formulation. The continuity equation from the formulated equations was finally modified by including a sink term for Budalang'i flood plain.

The sink term in this case referred to the term quantifying the difference between inflow and outflow and was noted as s_1. In the second objective, the study analysed the shallow water equations formulated for Budalang'i flood plain. Analysis entailed establishing the nature of flow and the stability condition based on the Froude number for the flood plain basin with the aide of Jacobian transformation. Using Nature of wave propagation and Froude number, alternative types of solutions were established.

In objective three, an explicit centered finite difference method was used to descritize the shallow water equations. Numerical approximations were followed with the adoption of Courant Friedrichs Lewy Condition for convergence. The use of

numerical approximations were carried out to enable appropriate simulations of the wave propagation in the Budalang'i flood plain using the Flood plain basin data. Simulations were carried out with the aide of Python program version 3.8. For effective simulations, varying depths were considered. Since the study accommodates both analytical part in objective one and two and numerical simulations in objective three, the methods were considered both analytical and numerical in modelling.

1.5.1   Area of Study

Budalang'i division lies on the shores of Lake Victoria, partly on the mouth of River Yala, but largely on the mouth of river Nzoia [27]. According to [14], River Nzoia is one of the largest rivers in western Kenya. The main stream of the river flows from the western side of the Elgeyo Escarpment and the Cherangani Hills from an elevation of approximately 2,286 m above mean sea level. It's tributaries, which flow from the high slopes of Mount Elgon, attain maximum elevation in the river's basin and are estimated at about 4,300 m above mean sea level. The tributaries in Mount Elgon include Kuywa, Sosio, Ewaso, Rogai and Koitobos. The catchment of river Yala has an estimated area of 3,351 km^2 and the River is one of the main rivers in Kenya draining into Lake Victoria. The river is approximated to be about 219 km long and it originates from the Nandi Escarpment water tower traversing Kakamega and Siaya counties as it flows downstream. The study basin has an annual average discharge of 28 m^3 s^{-1} [34]. The flood magnitudes have been estimated to be approximately an average of 2,367 m^3 s^{-1} to 3,881 m^3 s^{-1}. The upper reach is 135 m^2 to 257 m^2, with a slope of 1 to 240 which is approximated to be a percentage of 0.42. The middle reach is 20 km to 135 km with a slope of 1

to 390, approximated to be 0.26% and finally the lower reach is $10\,\mathrm{km}$ to $20\,\mathrm{km}$ with a slope of 1 to 3,400 which is approximately 0.03%. Approximately $110\,\mathrm{km}^2$ of the basin is usually affected by floods from Yala and Nzoia Rivers almost every year with an approximated flood depth of $0.5\,\mathrm{m}$ to $1\,\mathrm{m}$ lasting 20 to 30 days [20]. The lower River Nzoia and Yala (Budalang'i) basin was chosen because of its regional importance to agricultural crop production. It is also a flood prone basin and the rivers are the major tributaries to Lake Victoria. The area of the basin is approximated to $3,351\,\mathrm{km}^2$ with an average discharge approximately $28\,\mathrm{m}^3\,\mathrm{s}^{-1}$. During floods there is overtopping despite the building of the dykes as structural measures to curb flooding, leading to destruction of crops. Overtopping occurs as a result of sediment accumulation in the flood plain causing overbank flow and therefore resulting to floods [4].

1.5.2 Mathematical Model

The study formulated a $2D$ Shallow water model from the well known $3D$ Navier Stokes equations. The $2D$ shallow water model represents mass and momentum conservation, and is obtained by depth averaging the Navier Stokes equations [33]. The procedure eliminates from the beginning the free surface location problems which is now simply placed as the depth above the bottom surface. The momentum due to viscosity, turbulence and wind effects were neglected but coriolis terms were included in the model. Therefore the model can be written in differential conservation law form as a single vector equation. The main assumption of the shallow water model is that the horizontal length scale is much greater than the depth scale [8]. Thus, one can get rid of the vertical dimension by averaging the

mass and momentum conservation equations over the depth. The model can thus be written as,

$$\frac{\partial U}{\partial t} + \frac{\partial F(U)}{\partial x} + \frac{\partial G(U)}{\partial y} = S(U)$$

in which U is a variable vector and is a function of flood directions and time, that is x, y, t. F is the convective flux vector and G is the diffusive flux vector in the x and y directions respectively. S represents the source terms and the sink along the two momentum equations and the continuity equation respectively. The system describes the flow at time t where the height of the fluid at (x, y, t) are greater than 0, and finally, h denotes the water depth. Therefore the shallow water equation can also be written as in conservation form as

$$\frac{\partial h}{\partial t} + \frac{\partial hu}{\partial x} + \frac{\partial hv}{\partial y} = 0 \tag{1.3}$$

$$\frac{\partial hu}{\partial t} + \frac{\partial (hu^2 + \frac{1}{2}gh^2)}{\partial x} + \frac{\partial huv}{\partial y} = -gh\frac{\partial b}{\partial x} \tag{1.4}$$

$$\frac{\partial hv}{\partial t} + \frac{\partial huv}{\partial x} + \frac{\partial (hv^2 + \frac{1}{2}gh^2)}{\partial y} = -gh\frac{\partial b}{\partial y} \tag{1.5}$$

where u and v are the horizontal and vertical velocities respectively, and b represents the change in bed slope source term in the x or y directions. In the system, the $2D$ model allowed setting up of different conditions. For the initial conditions, initially dry and flood levels were taken to consideration. The initial boundary conditions were associated to the horizontal and vertical velocities where initially $u(x, y, 0) = f(x, y), \quad v(x, y, 0) = f(x, y) \quad (x, y) \in \Omega$ and $t = 0$. For the boundary conditions, free flow, wall and specified velocities were considered. Therefore $U(x, y, t) = g(x, y, t), (x, y) \in \Omega$ and $t > 0$ were treated as the boundary conditions. Even though the model is of the average type, a thin vertical elevation was

considered because $h > 0$, implying that the vertical to horizontal distance of the domain of wave travel is less than 1.

The following fundamental theorems were used in the study:

Theorem 1.5.1 (Leibnitz Rule)

Let $f(x, y)$ be a function where $f(x, y)$ and its partial derivative $f_x(x, y)$ are continuous in y and x in some region of the $(x - y)$ plane including $a(x) \leq y \leq b(x)$, $x_0 \leq x \leq x_1$. In addition, suppose the functions $a(x)$ and $b(x)$ are both continuous and both have continuous derivatives for $x_0 \leq x \leq x_1$. Then for an integral of the form

$$\int_{a(x)}^{b(x)} f(x, y) dy,$$

where $-\infty < a(x), b(x) < \infty$, the derivative of this integral is expressed as,

$$\frac{\partial}{\partial x} \left[\int_{a(x)}^{b(x)} f(x, y) dy \right] = f(x, b(x)).\frac{d}{dx} b(x) - f(x, a(x)).\frac{d}{dx} a(x) + \int_{a(x)}^{b(x)} \frac{\partial}{\partial x} f(x, y) dy,$$

where the partial derivative indicates that only the variation of $f(x, y)$ with x is considered in taking the derivative inside the integral.

Theorem 1.5.2 (Jacobian Transformation)

Let $x = g(u, v)$ and $y = h(u, v)$ indicate a transformation on the plane that is one to one from region S to region R. If h and g have continuous partial derivatives then the Jacobian of this transformation is,

$$\frac{\partial(x, y)}{\partial(u, v)} = \begin{vmatrix} \frac{\partial x}{\partial u} & \frac{\partial y}{\partial u} \\ \frac{\partial x}{\partial v} & \frac{\partial y}{\partial v} \end{vmatrix} = \frac{\partial x}{\partial u} \frac{\partial y}{\partial v} - \frac{\partial x}{\partial v} \frac{\partial y}{\partial u}$$

Therefore the Jacobian is simply the derivative of a coordinate transformation.

1.6   Significance of the Study

The solution of the flood wave Shallow water equations will be significant to meteorological stake-holders in flood mitigation. The results of this study can inform appropriate measures to reduce flood havoc in the study area. The findings may also aide flood disaster management stakeholders in determining risk in flood-prone areas to support decisions for risk management. Finally, the results will add more knowledge to the body of literature among scholars.

Chapter 2

Literature Review

Currently, there is rapid climate change due to ever increasing industrial activities, increase in population and clearance of indigenous forests in search for settlement worldwide [12]. This has increased the risks of droughts and floods, with the later affecting developing countries adversely [1]. Floods are a temporary inundation of water from the rivers, streams, lakes, oceans or flash floods onto lands not normally covered by water, and therefore have attracted scholarly studies in modeling [13]. This is also because extreme floods are characterised by unpredictable whether conditions, thus leading to shortfalls in the flood prediction systems in place [14]. In Kenya, historical flood occurrences has led to a comprehensive set up of flood mitigation strategies which have incurred the country a lot of finances [27]. For instance, in the year 2017, there were heavy downpours with inadequate preparedness in spite of the warning from the Kenya meteorological departments leading to the displacement of an estimated 800,000 people and death of approximately 300 people countrywide. Reports revealed that in Western Kenya, Busia and Siaya counties received most of the humanitarian needs due to prolonged rainfall with an estimated 35,000 people being affected as a result of displacement, [11]. Other counties that were affected were West Pokot, Garissa, Isiolo, Kisumu, Mandera, Marsabit,

Narok, Samburu, Taita-Taveta, Tana River, Turkana and Wajir [37]. In Western Kenya, floods have been occurring mainly in Budalang'i area in Busia County [16]. The major floods include the 1937, 1947, 1951, 1957, 1958, 1961, 1978, 1977 to 1978, El Nino, 2002, 2003, 2007 and 2009. During the 1997 to 1998 El nino, rainfall was 300 % of the normal with 12,000 people being displaced. The dykes were extensively damaged due to overtopping and breaching [34].

The Ministry of Water and Irrigation, through Kenya Meteorological departments came up with integrated flood management system [26]. The functional being the early flood warning system, which is a core component of flood mitigation that consists of real time monitoring, forecasting and dissemination of the warnings [30]. Other measures of flood mitigation in the area have included management of the catchment area, multipurpose dams, buildup of community based disaster management and making good use of flood waters [35] and [22]. Structural measures such as setting up of dykes to curb floods in the area have achieved a milestone success, leading to reduction in the displacement of people and extreme havoc previously caused by floods. However, the 2017 floods caused destruction of crops in the region, which are the main source of livelihood in the area [28]. Such a phenomenon was not expected, and implies that there is still much that needs to be done on flood propagation. Perhaps, a different approach can be applied in the flood mitigation. This gave a motivation to model the flood propagation using the shallow water equations.

Various studies have been carried out on the development of $2D$ shallow water equation among previous scholars. For instance, March[33] studied the derivation of a new two dimensional viscous shallow water model in rotating framework using asymptotic analysis while considering irregular topography, linear and quadratic bottom friction terms and capillary effects. This study formulated a new form

of the $2D$ equation with viscous effects, consistent with a previously formulated one dimensional equation by [18]. The results demonstrated that addition of a quadratic drag term with modified water depth dependent coefficients was coherent with the usual friction Manning-Chezy formulation used in oceanographic simulations.

Ferrari in [19] introduced appropriate scalings into a 3D anisotropic eddy viscosity model after averaging on the vertical direction and considering some asymptotic assumptions, and obtained a two-dimensional model. The study incorporated the motion of an incompressible fluid confined to a shallow basin with a slightly varying bottom topography. Coriolis force, surface wind and pressure stresses, together with bottom and lateral friction stresses were also taken into account. The derived model was found to be symmetrizable through a suitable change of variables. Numerical tests were also approximated with the aim to validate the proposed model.

Studies were carried out by [17] on the application of the depth averaged shallow water equations to several free surface flows in which the treatment of geometry introduced on the source terms and turbulence modelling were of interest. The convective flux was discretised with an hybrid scheme of upwind Godunovs schemes based on Roes average. The study established that fishway flows occurred which were highly turbulent and it had strong recirculation eddies which made it perfect model for turbulence tests but not an appropriate solution for shallow water model. Studies by [23] revealed modelling of shallow water equations using a high resolution $2D$ dam-break model with parallelization. Other techniques that have been used to solve the SWEs have highly adopted the upwind schemes. Among these techniques are the Volume of Fluid [30], Maker in cell [43], Finite Volume [31], high resolution Godunov-type scheme with finite volume [3] and volume of fluid methods [24] which did not give accurate results on the flood wave equation

and were limited to theoretical tests. A numerical model for the solution of the two-dimensional dam break problem developed in [45] was also based on second order approximate Riemann solver with a van Leer type limiter to solve the shallow water wave equation on a Cartesian grid. More recently, a study on the solution of shallow water equations was carried out by [2] on flood propagation with assumed grid. However, the current problem involves the structural measures such as dykes, which hold the water during flooding although the area encounters overtopping. This study sought to address the problem in Budalang'i flood plain.

Different studies that are related to modeling the flood phenomena in the study area include [26], who carried out the rainfall runoff modeling in Yala River Basin of Western Kenya. The study adopted the Geological stream flow and Muskingum Cunge models to model the hydrologic process of the River Yala network. The objective of this study was to come up with an early flood warning system to avoid the flood risk exposed to the downstream inhabitants. The findings indicated that the adopted tools were useful for issuing early flood warning message defined by peak stream flow and flood wave travel time. The study however concentrated on the stream flow routing whereas the most affected region are the downstream inhabitants, who mainly benefit from the flood basin. In addition, little was done on the flood wave dispersion thus without the knowledge of the frequency and wavelength, little can be known on the intensity of the hazard likely to happen in the event of a flood occurrence.

Flow Regime from International Experimental and Network Data (FRIEND) by [7] presented an appraisal study on suitable models that could be used in forecasting flows in the rivers of the Nile basin. In this appraisal study, systems and conceptual modeling techniques were applied to lake Victoria, Awash and the Blue Nile catchments. The models were applied in non-parametric and parametric

forms. Parameter optimization was carried out by ordinary least squares, Rosenbrock, Simplex and genetic algorithm. The rainfall which was the main input to these models was estimated using arithmetic mean. The findings revealed that in catchments which exhibit marked seasonal behaviour good results can be obtained with Linear Perturbation Model (LPM) which involved the assumption of linearity between the departures from seasonal expectations in input and output series. The application of the GFFS (collection of systems and conceptual models) software proved to be possible with variable efficiencies in the Nile River basin [20]. However, flood routing involving the wave propagation was not done under the conceptual models used. An almost similar work was also carried out by [38] who mainly indicated the challenges that were encountered in modeling the flow of Nile Rivers. Further work on flood routing techniques have also been reported in [9, 12, 25, 32, 39, 41, 42] but none of these studies have applied the $2D$ shallow water routing that pursues the wave dispersion and captures the variation of the depth and dry front effects as the wave propagates. Thus this study sought carry out mathematical modelling of flood wave in Budalang'i flood plain.

Chapter 3

Model Formulation, Analysis and Discussion

Model formulation entails depth averaging the Navier Stokes equations then applying the Leibnitz Rule. This is done with application to the Budalang'i flood plain while using the flood flow directions in the basin. The parameters governing the flood plain basin such as pressure, wind terms, vertical and horizontal velocities guide the formulation. Finally, a sink term is introduced to show the adjustment to most ideal formulated equations for the basin. Analysis of the shallow water model for the study domain entails obtaining the eigenvalues that eventually help determine the nature of flow. Finally, numerical simulation of the model is carried out using finite difference scheme.

3.1   Formulation of $2D$ flood wave model for Budalang'i Flood Plain

We consider the Navier Stokes equation,

$$\left(\frac{\partial u}{\partial x} + \frac{\partial v}{\partial y} + \frac{\partial w}{\partial z}\right) = 0$$

$$\rho\left(\frac{\partial u}{\partial t} + u\frac{\partial u}{\partial x} + v\frac{\partial u}{\partial y} + w\frac{\partial u}{\partial z}\right) = F_x - \frac{\partial p}{\partial x} + \left(\frac{\partial \tau_{xx}}{\partial x} + \frac{\partial \tau_{xy}}{\partial y} + \frac{\partial \tau_{zx}}{\partial z}\right)$$

$$\rho\left(\frac{\partial v}{\partial t} + u\frac{\partial v}{\partial x} + v\frac{\partial v}{\partial y} + w\frac{\partial v}{\partial z}\right) = F_y - \frac{\partial p}{\partial y} + \left(\frac{\partial \tau_{xy}}{\partial x} + \frac{\partial \tau_{yy}}{\partial y} + \frac{\partial \tau_{zy}}{\partial z}\right) \qquad (3.1)$$

$$\rho\left(\frac{\partial w}{\partial t} + u\frac{\partial w}{\partial x} + v\frac{\partial w}{\partial y} + w\frac{\partial w}{\partial z}\right) = F_z - \frac{\partial p}{\partial z} + \left(\frac{\partial \tau_{xz}}{\partial x} + \frac{\partial \tau_{yz}}{\partial y} + \frac{\partial \tau_{zz}}{\partial z}\right).$$

The stress state is represented as a symmetric tensor τ, whose components can be expressed in coordinate systems. The components of the velocity vector u, v, w align with the Cartesian- Coordinate directions (x, y, z). Such fluids are called Newtonian fluids. If we assume an incompressible fluid, the components of stress tensors can be expressed as follows,

$\tau_{xx} = -p + 2\mu\frac{\partial u}{\partial x} \quad \tau_{yy} = -p + 2\mu\frac{\partial v}{\partial y}, \quad \tau_{zz} = -p + 2\mu\frac{\partial w}{\partial z}$

$\tau_{xy} = \tau_{yx} = \mu\cdot\left(\frac{\partial u}{\partial y} + \frac{\partial v}{\partial x}\right), \quad \tau_{xz} = \tau_{zx} = \mu\cdot\left(\frac{\partial u}{\partial z} + \frac{\partial w}{\partial x}\right), \quad \tau_{yz} = \tau_{zy} = \mu\cdot\left(\frac{\partial w}{\partial y} + \frac{\partial v}{\partial z}\right),$

where μ is the coefficient of dynamic viscosity and p is the pressure term. We carry out integration of equation (3.1) using Leibnitz rule and later depth average. Since the shallow water equations are derived by applying a vertical averaging approach to the $3D$ Navier-Stokes equations shwon in system (3.1) under assumption of small vertical scale to horizontal scale, it is necessary to include the precipitation and infiltration terms in the resulting equation [44], as it ensures an appropriate accounting for the additional source terms to complete the model. Thus we start

with the continuity equation,

$$\frac{\partial u}{\partial x} + \frac{\partial v}{\partial y} + \frac{\partial w}{\partial z} = 0 \tag{3.2}$$

from equation (3.1) and integrate the individual terms over the vertical scale while taking the limits from the bottom of Budalang'i flood plain basin (bottom boundary) $(z = -h)$ to the surface water displacement of the basin (free surface elevation) (η). For the first term, we have,

$$\int_{-h}^{\eta} \frac{\partial u}{\partial x} dz = \frac{\partial}{\partial x} \int_{-h}^{\eta} u dz + u \mid_{z=-h} \frac{\partial(-h)}{\partial x} - u \mid_{z=\eta} \frac{\partial \eta}{\partial x}. \tag{3.3}$$

For the second term,

$$\int_{-h}^{\eta} \frac{\partial v}{\partial y} dz = \frac{\partial}{\partial y} \int_{-h}^{\eta} v dz + v \mid_{z=-h} \frac{\partial(-h)}{\partial y} - v \mid_{z=\eta} \frac{\partial \eta}{\partial y}. \tag{3.4}$$

For the third term

$$\int_{-h}^{\eta} \frac{\partial w}{\partial z} dz = w \mid_{z=\eta} - w \mid_{z=-h}. \tag{3.5}$$

Combining equations $(3.3) - (3.5)$ yields

$$\frac{\partial}{\partial x} \int_{-h}^{\eta} u dz + u \mid_{z=-h} \frac{\partial(-h)}{\partial x} - u \mid_{z=\eta} \frac{\partial \eta}{\partial x} +$$
$$\frac{\partial}{\partial y} \int_{-h}^{\eta} v dz + v \mid_{z=-h} \frac{\partial(-h)}{\partial y} - v \mid_{z=\eta} \frac{\partial \eta}{\partial y} + w \mid_{z=\eta} - w \mid_{z=-h} = 0 \tag{3.6}$$

which can be rearranged as shown in the equation (3.7)

$$\frac{\partial}{\partial x} \int_{-h}^{\eta} u dz + \frac{\partial}{\partial y} \int_{-h}^{\eta} v dz +$$

$$u \mid_{z=-h} \frac{\partial(-h)}{\partial x} + v \mid_{z=-h} \frac{\partial(-h)}{\partial y} - w \mid_{z=-h} - \quad (3.7)$$

$$u \mid_{z=\eta} \frac{\partial\eta}{\partial x} - v \mid_{z=\eta} \frac{\partial\eta}{\partial y} + w|_{z=\eta} = 0.$$

During flooding, the free surface becomes complex for the Budalang'i flood plain as observed by [1] and so the boundary becomes a moving boundary. This implies there is no relative normal flow and so by the condition of free surface, we have the change in free surface over time. Therefore velocity at free surface and bottom surface may be expressed as

$$\bar{w}|_{z=\eta} = \frac{D\eta}{Dt}|_{z=\eta} = \frac{\partial\eta}{\partial t} + \bar{u}|_{z=\eta} \frac{\partial\eta}{\partial x} + \bar{v}|_{z=\eta} \frac{\partial\eta}{\partial y}. \quad (3.8)$$

Now, in Budalang'i flood plain, the bottom is a material surface of the fluid and therefore not crossed by the flow and is stationary or impermeable, therefore this gives rise to another condition. We have $\bar{w}|_{z=-h} = \frac{D(-h)}{Dt}|_{z=-h} = \frac{\partial(-h)}{\partial t} + \bar{u}|_{z=-h}\frac{\partial(-h)}{\partial x} + \bar{v}|z = -h\frac{\partial(-h)}{\partial y}$. Rewriting the above and considering that $\frac{\partial(x,y)}{\partial t} = 0$, we have

$$u \mid_{z=-h} \frac{\partial(-h)}{\partial x} + v \mid_{z=-h} \frac{\partial(-h)}{\partial y} - w \mid_{z=-h} = 0, \quad (3.9)$$

from the second part of equation (3.7). Combining the first part of (3.7) and the left hand side (change in water surface elevation term) in equation (3.8), we end up with equation (3.10). First, we have $\left[\bar{u}\frac{\partial\eta}{\partial x} + \bar{v}\frac{\partial\eta}{\partial y} - \bar{w}\right] = \frac{\partial\eta}{\partial t}$ which is equation 3.8 and $\left[\bar{u}\frac{\partial(-h)}{\partial t} + \bar{v}\frac{\partial(-h)}{\partial y} - \bar{w}\right]_{z=-h} = 0$. Substituting these expressions into continuity

equation, we have,

$$\frac{\partial \eta}{\partial t} + \frac{\partial}{\partial x} \int_{-h}^{\eta} \bar{u}dz + \frac{\partial}{\partial y} \int_{-h}^{\eta} \bar{v}dz = 0. \tag{3.10}$$

Another geographical characteristic of Budalang'i flood plain is that the horizontal scale, $10,000\,\mathrm{km}$ is much larger than the vertical scale approximately $1.5\,\mathrm{m}$ during floods [26]. This implies that in the flood plain, the vertical momentum exchange is negligible as compared to the horizontal momentum exchange and so the vertical velocity component is much smaller than the horizontal velocity component. Thus the acceleration of movement of the flood waters in the vertical direction is negligible except acceleration due to gravity. Therefore, the pressure distribution over the vertical direction is hydrostatic and can be expressed as shown in the following equation, which is referred to as the hydrostatic pressure balance equation.

$$\frac{\partial p}{\partial z} = -\rho g. \tag{3.11}$$

Finally, we carry out depth averaging of equation (3.10) and employ the assumption of hydrostatic pressure as given by (3.11). In order to depth average, we consider the free surface of the water in the flood plain which is simply at $z = \eta$ and the bottom which is the water sediment interface at $z = -h$ and define two variables $\bar{u}$ and $\bar{v}$. Let $\bar{u}$ and $\bar{v}$ be the vertically averaged velocity vectors in the vertical of the horizontal components. Let also H be the total depth of the water, such that $H = h + \eta$. Then the averages on the vertical of the horizontal flood domain of the velocity vector can be expressed as equations (3.12) and (3.13)

below,

$$\bar{u} = \frac{1}{H} \int_{-h}^{\eta} u \, dz \tag{3.12}$$

$$\bar{v} = \frac{1}{H} \int_{-h}^{\eta} v \, dz. \tag{3.13}$$

These variables affirms the assumption that water flow in the vertical direction in the flood plain is small. Substituting the two variables, (3.12) and (3.13), in equation (3.10) yields depth averaged continuity equation (3.14)

$$\frac{\partial \eta}{\partial t} + \frac{\partial (H\bar{u})}{\partial x} + \frac{\partial (H\bar{v})}{\partial y} = 0 \tag{3.14}$$

which is the depth averaged form of the continuity equation.

We now formulate the depth averaged momentum equation for the shallow water system. First, we show that due to hydrostatic approach and constant density of the flood waters in the flood plain, pressure depends on η and the vertical coordinate while the horizontal pressure gradient depends on the free surface only. We only consider the right hand side term $\frac{\partial p}{\partial z}$ of the third momentum equation of system (3.1), which is simply the momentum equation in the z direction. This is partly because all the terms in the z direction of system (3.1) are small compared to the gravity and pressure terms and thus the equation reduces to equation (3.11). Integrating equation (3.11) from free surface at $z = \eta$ to some level z on the right hand side, we have,

$$\int_{p_s(x,y)}^{p(x,y,z)} dp = -\int_{\eta}^{z} \rho g \, dz,$$

where p_s is the pressure at the free surface, which simplifies to

$$p - p_s = -\rho g(z - \eta).$$

One of the assumptions made during flooding in the flood plain is that density is constant and so the pressure depends on the free surface and vertical coordinate. We thus have,

$$p - p_s = \rho g \eta - \rho g z \Rightarrow p = p_s + \rho g \eta - \rho g z.$$

After dividing the above expression through by $-\rho$ and obtaining the partial derivatives with respect to x we have the x-direction Reynolds equation below

$$\frac{-1}{\rho}\frac{\partial p}{\partial x} = \frac{-1}{\rho}\frac{\partial p_s}{\partial x} - g\frac{\partial \eta}{\partial x} + g\frac{\partial z}{\partial x}, \qquad (3.15)$$

where p_s is the pressure at the free surface. Therefore assuming that the surface pressure does not vary spartially, we have

$$\frac{-1}{\rho}\frac{\partial p}{\partial x} = -g\frac{\partial \eta}{\partial x},$$

in which s_o is the bottom slope given by $\frac{\partial z}{\partial x}$. Also, the horizontal pressure gradient in the flood plain depends on the free surface only

$$\frac{-1}{\rho}\frac{\partial p}{\partial x} = -g\frac{\partial \eta}{\partial x} \text{ and } \frac{-1}{\rho}\frac{\partial p}{\partial y} = -g\frac{\partial \eta}{\partial y}.$$

Assuming that the surface pressure does not vary then we have garvitation term as $-g\frac{\partial \eta}{\partial y}$ Adding the derived pressure gradients and dividing momentum equations in system (3.1) by ρ, the two momentum equations in the x and y directions can

thus be rewritten as follows,

$$\frac{\partial u}{\partial t} + u\frac{\partial u}{\partial x} + v\frac{\partial u}{\partial y} + w\frac{\partial u}{\partial z} = \frac{1}{\rho}F_x - g\frac{\partial \eta}{\partial x} + \frac{1}{\rho}\frac{\partial \tau_{xx}}{\partial x} + \frac{1}{\rho}\frac{\partial \tau_{xy}}{\partial y} + \frac{1}{\rho}\frac{\partial \tau_{zx}}{\partial z}$$
$$\frac{\partial v}{\partial t} + u\frac{\partial v}{\partial x} + v\frac{\partial v}{\partial y} + w\frac{\partial v}{\partial z} = \frac{1}{\rho}F_y - g\frac{\partial \eta}{\partial y} + \frac{1}{\rho}\frac{\partial \tau_{xy}}{\partial x} + \frac{1}{\rho}\frac{\partial \tau_{yy}}{\partial y} + \frac{1}{\rho}\frac{\partial \tau_{zy}}{\partial z}. \tag{3.16}$$

Consider the left hand side of the x -momentum equation (3.16). In order to change the terms in the left hand side of the momentum equations (3.16) from non-conservative to conservative form, we add $\bar{u}$ times the continuity equation to equation (3.16) and obtain the following terms

$$\frac{\partial \bar{u}}{\partial t} + \bar{u}\frac{\partial \bar{u}}{\partial x} + \bar{v}\frac{\partial \bar{u}}{\partial y} + \bar{w}\frac{\partial \bar{u}}{\partial z} + \bar{u}\frac{\partial \bar{u}}{\partial x} + \bar{u}\frac{\partial \bar{v}}{\partial y} + \bar{u}\frac{\partial \bar{w}}{\partial z} = \frac{1}{\rho}F_x - g\frac{\partial \eta}{\partial x} + \frac{1}{\rho}\frac{\partial \tau_{xx}}{\partial x} + \frac{1}{\rho}\frac{\partial \tau_{xy}}{\partial y} + \frac{1}{\rho}\frac{\partial \tau_{zx}}{\partial z}$$

which on simplification yields equation (3.17) below.

$$\frac{\partial u}{\partial t} + \frac{\partial u^2}{\partial x} + \frac{\partial (uv)}{\partial y} + \frac{\partial (uw)}{\partial z} = 0. \tag{3.17}$$

Next, vertically averaging these equations and integrating each term with respect to z and apply the Leibnitz Rule

$$\int_{-h}^{\eta} \frac{\partial u}{\partial t}dz = \frac{\partial}{\partial t}\int_{-h}^{\eta} udz + u|_{z=-h}\frac{\partial (-h)}{\partial t} - u|_{z=\eta}\frac{\partial \eta}{\partial t}$$
$$\int_{-h}^{\eta} \frac{\partial u^2}{\partial x}dz = \frac{\partial}{\partial x}\int_{-h}^{\eta} u^2dz + u^2|_{z=-h}\frac{\partial (-h)}{\partial x} - u^2|_{z=\eta}\frac{\partial \eta}{\partial x}$$
$$\int_{-h}^{\eta} \frac{\partial (uv)}{\partial y}dz = \frac{\partial}{\partial y}\int_{-h}^{\eta} uvdz + uv|_{z=-h}\frac{\partial (-h)}{\partial y} - uv|_{z=\eta}\frac{\partial \eta}{\partial y}$$
$$\int_{-h}^{\eta} \frac{\partial (uw)}{\partial z}dz = uw|_{z=\eta} - uw|_{z=-h} \tag{3.18}$$

Combining the four equations on the left hand side of equation 3.18, and the right hand side we have the equations in system (3.19)

$$
\begin{aligned}
&\int_{-h}^{\eta} \left[\frac{\partial u}{\partial t} + \frac{\partial u^2}{\partial x} + \frac{\partial(uv)}{\partial y} + \frac{\partial(uw)}{\partial z} \right] \\
&= \frac{\partial}{\partial t} \int_{-h}^{\eta} u\, dz + \frac{\partial}{\partial x} \int_{-h}^{\eta} u^2 dz + \frac{\partial}{\partial y} \int_{-h}^{\eta} uv\, dz \\
&\quad - u|_{z=\eta} \left[\frac{\partial \eta}{\partial t} + u|_{z=\eta} \frac{\partial \eta}{\partial x} + v|_{z=\eta} \frac{\partial \eta}{\partial y} - w|_{z=\eta} \right] + \\
&u|_{z=-h} \left[\frac{\partial(-h)}{\partial t} + u|_{z=-h} \frac{\partial(-h)}{\partial x} + v|_{z=-h} \frac{\partial(-h)}{\partial y} - w|_{z=-h} \right].
\end{aligned}
\tag{3.19}
$$

By using conditions in equations (3.8),(3.9),(3.12), and (3.13) we have, from system (3.19),

$$
-\frac{\partial \eta}{\partial t} = u|_{z=\eta} \frac{\partial \eta}{\partial x} + v|_{z=\eta} \frac{\partial \eta}{\partial y} - w|_{z=\eta},
$$

$$
\frac{\partial(-h)}{\partial t} = 0,
\tag{3.20}
$$

since there is no change in bottom surface, and finally

$$
u|_{z=-h} \frac{\partial(-h)}{\partial t} + u|_{z=-h} \frac{\partial(-h)}{\partial x} + v|_{z=-h} \frac{\partial(-h)}{\partial y} - w|_{z=-h} = 0,
$$

indicating the solid bottom such that the bottom is a material surface of the fluid not crossed by the flow and is stationary, implying that there is no normal flow thus zero result. Therefore the x momentum equation is simplified to,

$$
\frac{\partial}{\partial t} \int_{-h}^{\eta} u\, dz + \frac{\partial}{\partial x} \int_{-h}^{\eta} u^2 dz + \frac{\partial}{\partial y} \int_{-h}^{\eta} uv\, dz = \frac{\partial H\bar{u}}{\partial t} + \frac{\partial(H\bar{u}^2)}{\partial x} + \frac{\partial(H\bar{u}\bar{v})}{\partial y}.
\tag{3.21}
$$

Budalang'i flood plain lies near the equatorial line and therefore the consideration of the possible significance of the coriolis term is important. The coriolis parameter represents the force exerted to a body in rotating frame and is more significant

near the equatorial regions [13]. We thus introduce the coriolis term fv whereby $f = 2\rho\nu\sin\theta$ is the coriolis parameter, ω is the angular velocity of the earth, θ is the latitude. Taking note of this, we now integrate each term of the right hand side of the x-momentum equation of system (3.16) with respect to z after rearranging and also rewrite the vector of volume forces as

$$\overrightarrow{F} = \begin{pmatrix} 2\rho\omega\nu\sin\theta \\ -2\rho\omega\upsilon\sin\theta \\ -\rho g \end{pmatrix}$$

for volume forces $F_x = 2\rho\omega\nu\sin\theta$, $F_y = -2\rho\omega\upsilon\sin\theta$, and $F_z = -\rho g$, if only the Coriolis and gravitational forces are accounted for as follows in system (3.22).

$$-\int_{-h}^{\eta} g\frac{\partial\eta}{\partial x}dz = -g\left[\frac{\partial}{\partial x}\int_{-h}^{\eta}\eta dz - \eta|_{z=\eta}\frac{\partial\eta}{\partial x} + \eta|_{z=-h}\frac{\partial(-h)}{\partial x}\right],$$

$$\int_{-h}^{\eta}\left[\frac{1}{\rho}\frac{\partial\tau_{xx}}{\partial x} + \frac{1}{\rho}\frac{\partial\tau_{xy}}{\partial y} + \frac{1}{\rho}\frac{\partial\tau_{zx}}{\partial z}\right]dz$$

$$= \frac{1}{\rho}\frac{\partial}{\partial x}\int_{-h}^{\eta}\tau_{xx}dz + \frac{1}{\rho}\frac{\partial}{\partial y}\int_{-h}^{\eta}\tau_{yx}dz - \frac{1}{\rho}\left[\tau_{xx}\frac{\partial\eta}{\partial x} + \tau_{yx}\frac{\partial\eta}{\partial y} - \tau_{zx}\right]_{z=\eta} + \tag{3.22}$$

$$\frac{1}{\rho}\left[\tau_{xx}\frac{\partial(-h)}{\partial x} + \tau_{yx}\frac{\partial(-h)}{\partial y} - \tau_{zx}\right]_{z=-h},$$

$$\int_{-h}^{\eta}\frac{1}{\rho}F_x dz = \frac{1}{\rho}\int_{-h}^{\eta}(2\rho\omega\nu\sin\theta)dz = fH\bar{\upsilon}.$$

Since we have no slip conditions at the bottom surface in the flood plain, then $u = v = w = 0$. Also, applying the boundary condition by performing stress balance at the Budalang'i flood plain surface, the equations of the wind stress and bottom stress are expressed as,

$$-\left[\tau_{xx}\frac{\partial\eta}{\partial x} + \tau_{yx}\frac{\partial\eta}{\partial y} - \tau_{zx}\right]_{z=\eta} = -\tau_x^s, \tag{3.23}$$

where $\frac{\tau_x^s}{\rho}$ is applied surface stress. Similarly, the equation of bottom stress are expressed as,

$$- \left[\tau_{xx} \frac{\partial(-h)}{\partial x} + \tau_{yx} \frac{\partial(-h)}{\partial y} - \tau_{zx} \right]_{z=-h} = \tau_x^b. \tag{3.24}$$

Finally, the x-momentum equation from equations (3.16) can be expressed as follows,

$$\begin{aligned}
\frac{\partial u}{\partial t} + u\frac{\partial u}{\partial x} + v\frac{\partial u}{\partial y} + w\frac{\partial u}{\partial z} = \\
-g\frac{\partial}{\partial x} \int_{-h}^{\eta} \eta dz + g\eta|_{z=\eta}\frac{\partial \eta}{\partial x} - g\eta|_{z=-h}\frac{\partial(-h)}{\partial x} + \\
\frac{1}{\rho}H\frac{\partial \bar{\tau}_{xx}}{\partial x} + \frac{1}{\rho}H\frac{\partial \bar{\tau}_{yx}}{\partial y} - \frac{\tau_x^b}{\rho} + \frac{\tau_x^s}{\rho} + fH\bar{v}.
\end{aligned} \tag{3.25}$$

Expanding gravity related terms we have

$$-g\frac{\partial}{\partial x} \int_{-h}^{\eta} \eta dz = -g\eta \int_{-h}^{\eta} dz = -g\frac{\partial(\eta H)}{\partial x},$$

and applying chain rule for the first three terms of the right hand side of equation (3.24) as follows,

$$\begin{aligned}
-g\frac{\partial(\eta H)}{\partial x} + g\eta\frac{\partial \eta}{\partial x} - g\eta\frac{\partial(-h)}{\partial x} = \\
-\eta g\frac{\partial(H)}{\partial x} - gH\frac{\partial(\eta)}{\partial x} + g\eta\frac{\partial \eta}{\partial x} - g\eta\frac{\partial(-h)}{\partial x} = \\
g\left[\eta\frac{\partial(H)}{\partial x} - H\frac{\partial(\eta)}{\partial x} + \eta\frac{\partial \eta}{\partial x} + \eta\frac{\partial(h)}{\partial x} \right] \\
= -gH\frac{\partial \eta}{\partial x},
\end{aligned}$$

the right hand side of the x momentum equation of system (3.16) becomes

$$-gH\frac{\partial \eta}{\partial x} + \frac{1}{\rho}H\frac{\partial \bar{\tau}_{xx}}{\partial x} + \frac{1}{\rho}H\frac{\partial \bar{\tau}_{yx}}{\partial y} - \frac{\tau_x^b}{\rho} + \frac{\tau_x^s}{\rho} + fH\bar{v}. \tag{3.26}$$

Performing a similar operation for the y-direction and including the sink term s_1 which is gain or loss through inflow, outflow, evaporation and infiltration to the equations, the overall form of the depth averaged equation can be written as follows,

$$\frac{\partial \eta}{\partial t} + \frac{\partial(H\bar{u})}{\partial x} + \frac{\partial(H\bar{v})}{\partial y} = s_1 \tag{3.27}$$

$$\frac{\partial H\bar{u}}{\partial t} + \frac{\partial(H\bar{u}^2)}{\partial x} + \frac{\partial H\bar{u}\bar{v}}{\partial y} - fH\bar{v} = -gH\frac{\partial \eta}{\partial x} + H\frac{1}{\rho}\frac{\partial \bar{\tau}_{xx}}{\partial x} + \frac{1}{\rho}\frac{\partial \bar{\tau}_{xy}}{\partial y} - \frac{1}{\rho}\tau_x^b + \frac{1}{\rho}\tau_x^s \tag{3.28}$$

$$\frac{\partial H\bar{v}}{\partial t} + \frac{\partial(H\bar{u}\bar{v})}{\partial x} + \frac{\partial H\bar{v}^2}{\partial y} + fH\bar{u} = -gH\frac{\partial \eta}{\partial y} + H\frac{1}{\rho}\frac{\partial \bar{\tau}_{yy}}{\partial y} + \frac{1}{\rho}\frac{\partial \bar{\tau}_{xy}}{\partial y} - \frac{1}{\rho}\tau_y^b + \frac{1}{\rho}\tau_y^s \tag{3.29}$$

For simplicity purposes, we divide through by H and ignore the surface shear stress, bottom shear stress and the stress tensor components in the momentum equations since they are negligible in the study domain as they can be applicable over domains that are over $100{,}000\,\text{km}^2$ while our study is only $3{,}351\,\text{km}^2$ [19]. For the continuity equation, we let $H = \eta + h$. Also, considering the mean flow velocities and putting u, v instead of $\bar{u}, \bar{v}$ the resulting system of shallow water equations can therefore be written as

$$\frac{\partial \eta}{\partial t} + \frac{\partial u(\eta + h)}{\partial x} + \frac{\partial v(\eta + h)}{\partial y} = s_1 \tag{3.30}$$

$$\frac{\partial u}{\partial t} + \frac{\partial u^2}{\partial x} + \frac{\partial(uv)}{\partial y} - fv = -g\frac{\partial \eta}{\partial x} \tag{3.31}$$

$$\frac{\partial v}{\partial t} + \frac{\partial(uv)}{\partial x} + \frac{\partial v^2}{\partial y} + fu = -g\frac{\partial \eta}{\partial y} \tag{3.32}$$

3.2   Analysis of Shallow water equations for Budalang'i Flood Plain

Rewriting the two momentum equations (3.30) to (3.32) in primitive form for simplicity purpose, we have,

$$\frac{\partial \eta}{\partial t} + \frac{\partial}{\partial x}[(\eta + h)u] + \frac{\partial}{\partial y}[(\eta + h)v] = s_1 \tag{3.33}$$

$$\frac{\partial u}{\partial t} + u\frac{\partial u}{\partial x} + v\frac{\partial u}{\partial y} - fv + g\frac{\partial \eta}{\partial x} = 0 \tag{3.34}$$

$$\frac{\partial v}{\partial t} + u\frac{\partial v}{\partial x} + v\frac{\partial v}{\partial y} + fu + g\frac{\partial \eta}{\partial y} = 0. \tag{3.35}$$

From these shallow water equations, analysis entailed establishing the nature of flow and the stability condition based on the Froude number. Budalang'i flood plain is known to have rapid flows leading to destruction of properties around the adjacent domain of floods. Classifying the flow attenuation or amplification was of paramount importance. The equations are therefore transformed for analysis. From the above equations, two matrices can be formed. We apply the Jacobian Transformation as follows,

Let (3.33) be f_1, (3.33) be f_2 and (3.34) be f_3.

We obtain the partial derivative of free surface elevation (η), vertically averaged velocity u and horizontally averaged velocity v for each of the three functions with respect to x and y starting with the x term as follows,

$$f'(x) = \begin{vmatrix} \partial\frac{\partial f_{1\eta}}{\partial x} & \frac{\partial f_{1u}}{\partial x} & \frac{\partial f_{1v}}{\partial x} \\ \partial\frac{\partial f_{2\eta}}{\partial x} & \frac{\partial f_{2u}}{\partial x} & \frac{\partial f_{2v}}{\partial x} \\ \partial\frac{\partial f_{3\eta}}{\partial x} & \frac{\partial f_{3u}}{\partial x} & \frac{\partial f_{3v}}{\partial x} \end{vmatrix} = \begin{bmatrix} u & \eta + h & 0 \\ g & u & 0 \\ 0 & 0 & u \end{bmatrix}.$$

We repeat the same process for the y term and end up with two matrices, that is, matrix A and B corresponding to the vectors of conserved variables in the x and y directions respectively as follows,

$$A = f'(x) = \begin{bmatrix} u & \eta + h & 0 \\ g & u & 0 \\ 0 & 0 & u \end{bmatrix} \text{ and } B = g'(x) = \begin{bmatrix} v & 0 & \eta + h \\ 0 & v & 0 \\ g & 0 & v \end{bmatrix}. \qquad (3.36)$$

and let I be the identity matrix

$$I = \begin{bmatrix} 1 & 0 & 0 \\ 0 & 1 & 0 \\ 0 & 0 & 1 \end{bmatrix} \qquad (3.37)$$

According to [40], computation of stability for flow parameters may entail assessing the Froude number. The approach used was computing the eigenvalues that aided in the calculation of the Froude number. Studies by [40] also indicates that the nature of wave propagation depends on the Froude number. Now, starting with the x-direction, we find the eigenvalues of matrix A using the characteristic equation $\mid A - \lambda I \mid = 0$, that is,

$$\begin{vmatrix} u - \lambda & \eta + h & 0 \\ g & u - \lambda & 0 \\ 0 & 0 & u - \lambda \end{vmatrix} = 0, \qquad (3.38)$$

and obtain the following characteristic equation

$$(u - \lambda)\left[(u - \lambda)(u - \lambda)\right] - (\eta + h)\left[g(u - \lambda)\right] = 0, \qquad (3.39)$$

whose solution is

$$\lambda_1^* = u$$
$$\lambda_2^* = u + \sqrt{g(\eta + h)}$$
$$\lambda_3^* = u - \sqrt{g(\eta + h)}.$$

Repeating the same analysis for the y direction, we obtain the following eigenvalues

$$\lambda_1 = v$$
$$\lambda_2 = v + \sqrt{g(\eta + h)}$$
$$\lambda_3 = v - \sqrt{g(\eta + h)}.$$

Since these eigenvalues are real and distinct, the shallow water equations are hyperbolic partial differential equations [36]. Therefore the equations admit discontinuous weak solutions [36], which could be a 'sink' and gives an approximate of a breaking wave in the flood plain. However, such a wave may be extremely small and negligible. The eigenvalues take the form of a convective velocity minus/plus a phase velocity. Dividing convective by phase yields a Froude number, for each x- and y-direction [6], which is practical for the flood plain. The Froude number may be thought of as a relation of inertia to gravitational forces: the top term being related to kinetic energy, the bottom to potential energy. Flows with Froude numbers less than one are said to be subcritical, and flows with Froude number greater than one are said to be supercritical. During floods, the convective velocity implies the surface waves which is usually more faster than the phase velocity which is slower since initially the flood plain was dry and consequent rains and inflow leads to increase in water depth before rapid generation of surface waves. Dividing the convective velocity by phase velocity yields a Froude number for each of the two

directions which are

$$\frac{u^2}{gH} = Fr_x^2 \tag{3.40}$$

$$\frac{v^2}{gH} = Fr_y^2 \tag{3.41}$$

indicating a relation of inertia to gravitational forces. As result of more rapid surface waves during consistent rains, the resulting phenomena leads to supercritical flows. The initial subcritical flows fades with time and eventually we have rapid supercritical flows in this case. More specifically, in Budalangi plain, the average discharge has been measured to have an average of $30\,\mathrm{m^3\,s^{-1}}$ [26] which corresponds to the potential discharge of the water flow in the basin. However, with continued rains, the surface discharge has been estimated to be 3 times more than the potential discharge [27]. Thus we have

$$\frac{90\,\mathrm{m^3\,s^{-1}}}{30\,\mathrm{m^3\,s^{-1}}} = 3 \tag{3.42}$$

implying that $Fr_x^2 > 1$, which is a large Froude number implying that there are rapid supercritical flows leading to adverse effects of unstable flood waves. However, the horizontal velocities do not vary with depth and thus the non linear terms are eliminated. This is accomplished through linearization of the two momentum equations for a more appropriate solution. It is also impossible to obtain complete analytic solutions from such analysis, therefore according to [22], thus the best numerical simulation can be obtained by linearizing the two momentum equations while the continuity equation solved in non linear form. To carry out linearization, we let $u = \zeta + \acute{u}, \quad v = \xi + \acute{v}$ and $\eta = \varrho + \acute{\eta}$ in which the capital letters indicates the averages and the primes indicate the perturbations. We substitute these variables

in equation (3.43) to (3.46) as follows,

$$\frac{\partial \varrho + \acute{\eta}}{\partial t} + \frac{\partial}{\partial x}[(\varrho + \acute{\eta} + h)(\zeta + \acute{u})] + \frac{\partial}{\partial y}[(\eta + h)(\xi + \acute{v})] = s_1 \tag{3.43}$$

$$\frac{\partial(\zeta + \acute{u})}{\partial t} + u\frac{\partial(\zeta + \acute{u})}{\partial x} + v\frac{\partial(\zeta + \acute{u})}{\partial y} - f(\xi + \acute{v}) + g\frac{\partial(\varrho + \acute{\eta})}{\partial x} = 0 \tag{3.44}$$

$$\frac{\partial(\xi + \acute{v})}{\partial t} + (\zeta + \acute{u})\frac{\partial(\xi + \acute{v})}{\partial x} + v\frac{\partial(\xi + \acute{v})}{\partial y} + fu + g\frac{\partial(\varrho + \acute{\eta})}{\partial y} = 0. \tag{3.45}$$

Furthermore we let $V = U = 0$ and drop the prime terms for assumption of linearization. Finally, we end up with linearized shallow water equation appropriate for numerical simulation as follows.

$$\frac{\partial \eta}{\partial t} + \frac{\partial u(\eta + h)}{\partial x} + \frac{\partial v(\eta + h)}{\partial y} = s_1 \tag{3.46}$$

$$\frac{\partial u}{\partial t} - fv = -g\frac{\partial \eta}{\partial x} \tag{3.47}$$

$$\frac{\partial v}{\partial t} + fu = -g\frac{\partial \eta}{\partial y}. \tag{3.48}$$

Equations (3.46) to (3.48) were therefore approximated numerically using finite difference under numerical simulation.

3.3   Simulations of $2D$ Shallow water model for Budalang'i flood plain

System (3.30) to (3.32) is solved numerically using finite difference scheme.There are many techniques for numerical approximations, however, Finite differences are by far the easiest numerical method to understand and implement when tackling differential equations, particularly $2D$ Shallow water equations, for problems that satisfy its structured discretization assumptions, and can be found to be useful in any domain when estimation of derivatives is needed[5]. Unlike other numerical methods, it is more flexible when approximating dynamic fluid such as flood flows. For stability, Courant Friedrichs Lewy Condition CFL was used. According to [13], the Courant number for $2D$ shallow water equations can be defined from CFL as follows,

$$C = \Delta t \left(\sqrt{gH} + V_{max} \right) \left(\frac{1}{\Delta x^2} + \frac{1}{\Delta y^2} \right)^{\frac{1}{2}},$$

where C refers to the Courant number. Therefore using the stability condition $CFL < 1$ from the Courant number defined above, an optimal stability criteria according to [29] is obtained as follows for optimal time step,

$$\Delta t \leq \frac{\Delta x \Delta y}{(\sqrt{gH_{max}})\sqrt{(\Delta x^2 + \Delta y^2)}}. \tag{3.49}$$

Where Δt is the time increment, Δx and Δy are the grid spacing in the x and y directions respectively and g is the acceleration due to the gravity. $\sqrt{gH}$ is the magnitude of velocity. Acceleration due to gravity is measured at $9.81\,\mathrm{m\,s^{-2}}$. The velocity components of the boundary were set to zero. In addition, f, which is the Coriolis force, is approximated to 0.00005 along the equatorial regions, [4]. The

shallow water equations were discretized using explicit centered finite difference in space starting with the continuity equation following [5]. Therefore the derivatives of partial differential equations were approximated by linear combination of function values at grid points in the domain $\Omega = (0, X)$ at $u_i \simeq u(x_i)$ where $i = 1, 2, 3, ..., N$. $x_i = i \triangle x$ with meshsize as $\triangle x = \frac{X}{N}$. The first order derivative is given as,

$$\frac{\partial u}{\partial x}(\bar{x}) = lim_{x \to 0} \frac{u(\bar{x} + \Delta x) - u(\bar{x})}{\Delta x} = lim_{x \to 0} \frac{u(\bar{x}) - u(\bar{x} - \Delta x)}{\Delta x}$$
$$= lim_{x \to 0} \frac{u(\bar{x} + \Delta x) - u(\bar{x} - \Delta x)}{2\Delta x}$$

from which we use the Taylor series expansion,

$$\Sigma_{n=0}^{\infty} \frac{(x - x_i)^n}{n!} \left(\frac{\partial^n u}{\partial x^n} \right)_i , u \subset \Omega$$

then we have the first approximation of forward difference as

$$T_1 = u_{i+1} = u_i + \Delta x (\frac{\partial u}{\partial x})_i + \frac{(\Delta x)^2}{2} \left(\frac{\partial^2 u}{\partial x^2} \right)_i + \frac{(\Delta x)^3}{6} \left(\frac{\partial^3 u}{\partial x^3} \right)_i + ...$$
$$T_2 = u_{i-1} = u_i - \Delta x (\frac{\partial u}{\partial x})_i + \frac{(\Delta x)^2}{2} \left(\frac{\partial^2 u}{\partial x^2} \right)_i - \frac{(\Delta x)^3}{6} \left(\frac{\partial^3 u}{\partial x^3} \right)_i + ...$$

Subtracting $T_1 - T_2$ and ignoring the higher order terms which form the error, we get the first order centered finite difference approximation of vertical velocity with respect to x partial derivative as follows,

$$\left(\frac{\partial u}{\partial x} \right)_i = \frac{u_{i+1} - u_{i-1}}{2\Delta x}.$$

For the shallow water equations, a partial derivative at point x_i, that is $\frac{\partial u_j}{\partial x}$ can thus be expressed as,

$$\frac{\partial u_j}{\partial x} \simeq \frac{u_{i+1} - u_{i-1}}{2\Delta x}$$

The initial conditions are a disturbance from water inflow causing a gaussian bump indicated by flow of water into the basin as shown in Figure 3.1 front right corner, with velocity greater than 0.
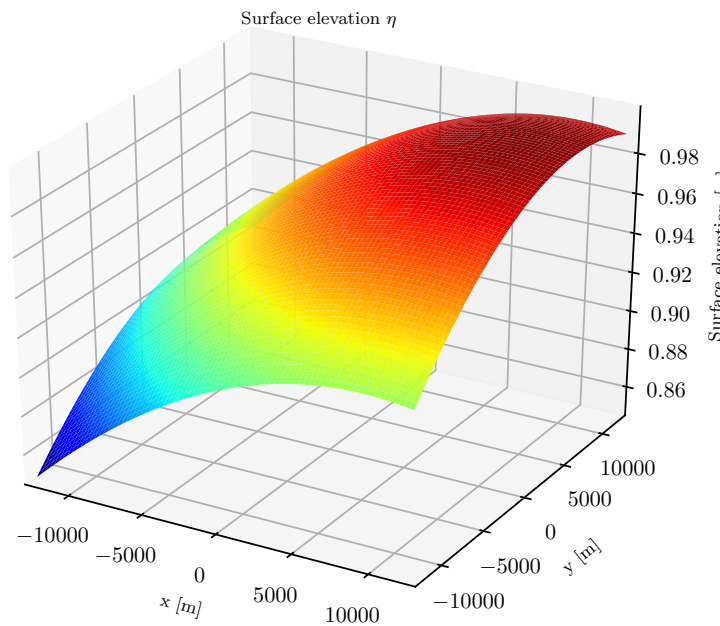
Figure 3.1: Initial wave

Figure 3.1 shows the gravity wave in flow direction from the disturbance of the water in the basin. The Figure shows the horizontal velocity evolving and finally, there is decay of the wave away from the initial inception causing dispersion in different directions. The evolution depends on time and this is further illustrated in the same Figure 3.1. Initially, the water was assumed to be at rest and while the boundaries were set to wall boundaries. Suddenly after a short time, water started to move in all directions. As time increases the circular shock waves propagated outwards, whereas the circular rarefaction wave traveled inwards showing that this

wave almost reaches the center of the domain. This phenomenon continued until the rarefaction wave has fully plunged into the center of the domain and this wave was suddenly reflected creating a sharp gradient of water surface elevation.

As the heavy down pour continues, there is increased generation of waves due to water increase. Wave propagation becomes unstable and therefore the frequency increases. Increased frequency and amplitude is also contributed by increased bottom friction due to dispersion of the waves across the banks, as well as sedimentation that perviously occurred.
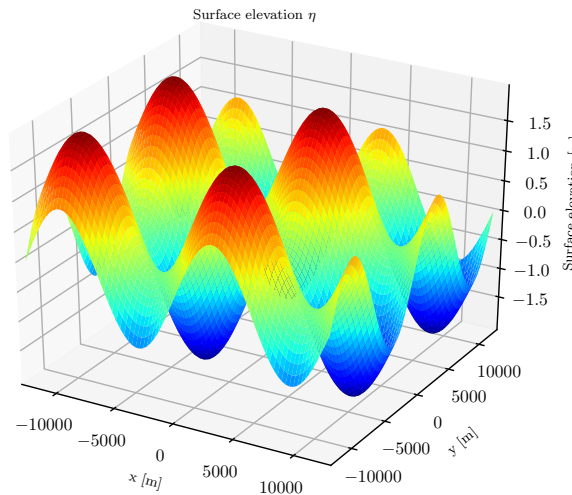
Figure 3.2: Turbulence

There is also an indication of turbulence of the waves showing that at the peak of the inflow, there is likelihood of breaking of waves with shocks and increased turbulence. This happens with evolution of time during the heavy rains, implying that the flood phenomena in Budalang'i area is mainly dependent on the high frequency waves that results to turbulence. These results could be similar to experimental results obtained by other studies [40].

The presence of dykes shows initial resistance to water increase. However, due to earlier perceived sedimentation, flood waters overflows the dykes which causes overbank burst and therefore renders the dykes of little use [26].
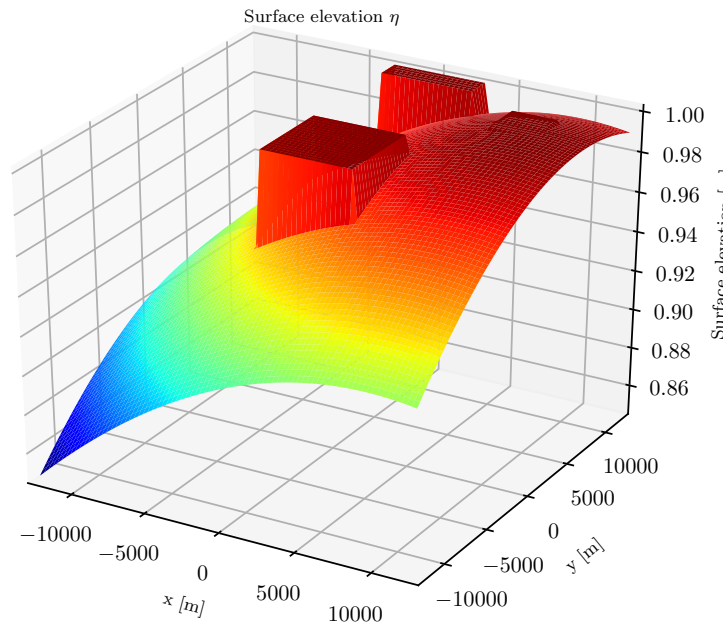
Figure 3.3: Overbank Flow

This scenario indicates that the presence of dykes is of importance though not permanent. The two blocks shown in Figure 3.3 indicates that water overflows the dykes leading to eventual coverage. Waves therefore keep dispersing away from the initial point resulting to floods in the surrounding area. This is a typical scenario in Budalang'i flood plain where dykes have been previously erected with some little help [28]. As a result of long rains, dykes are submerged by the increasing amount of water leading to overbank flow.

As a result of increased turbulence with greater energy of the shallow water waves, dykes were submerged leading to overbank flow. Therefore a sink was introduced. Sink in this case indicates the amount of water that either infiltrates underground or bore holes within the basin of the study. Similarly, the quantity eliminated that compares to the amount of sedimentation represented the sinks.
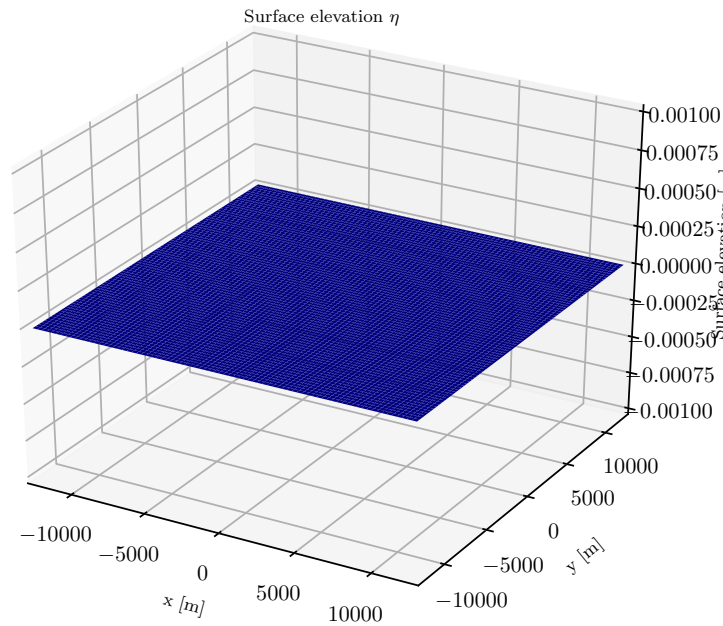
Figure 3.4: Final Water Level due to Sink

Figure 3.4 indicates that after introduction of the sink term, there is reduced level of water the basin of the study. The reduced gravity waves loses most of the energy due to removed sedimentation leading to reduction of the water level. With time evolution, there is further indication of convergence to steady state of the waves. However, as shown, there is reduced amount of water. This shows that a sink is very important to the control of the floods and with accurate approximation, it could reduce the flooding effect in the area of the study.

As a result of the introduced sink term, the water level reduces and therefore the wave velocity declines back to almost zero velocity. This is shown in Figure 3.5 that follows. The flow direction remains as shown by the arrows.
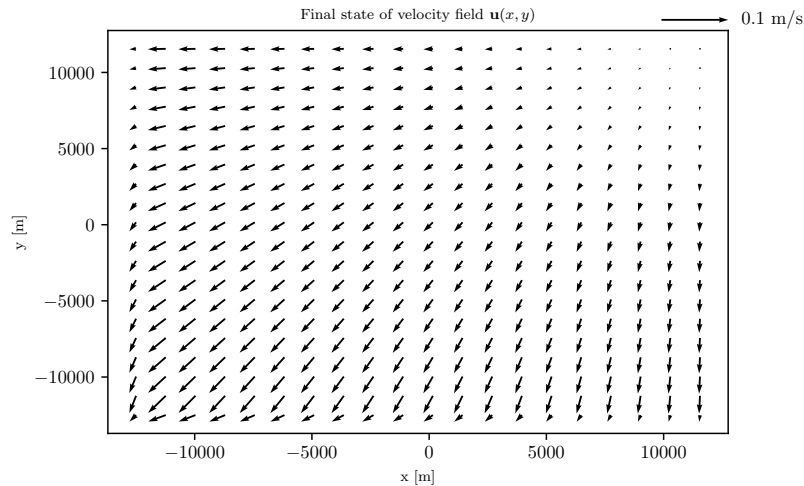
Figure 3.5: Steady State Velocity

Given more time the circular shock wave propagated further outwards from the domain center as shown in Figure 3.5. The primary circular waves are seen to propagate outwards although with high decay of damping factor and interestingly, the secondary circular shock wave that had recently been created traveled towards that center. As time increases, it is shown that the primary circular wave almost reached the domain boundary and at this time a very small gradient of water surface elevation had been created near that boundary. On the other hand, reflection of the secondary waves increases leading to a steady state situation of velocity. There is reduced primary as well as secondary waves due to reduced energy.

The second system of shallow water equations to be solved entailed the linearized shallow water equations. This was carried out in order to compare the two types of solutions. After linearization, the resulting equations are described in objective two. This equations takes into consideration the effect of coriolis term as well as the rotation of the earth.

The height field is set with an initial condition of disturbance caused by water inflow into the basin resulting to generation of waves. As the equations evolve, the velocities, u and v are induced and gravity waves starts radiating outwards from the initial disturbance. Figure 3.6 shows gravity waves radiating away from the initial disturbance.
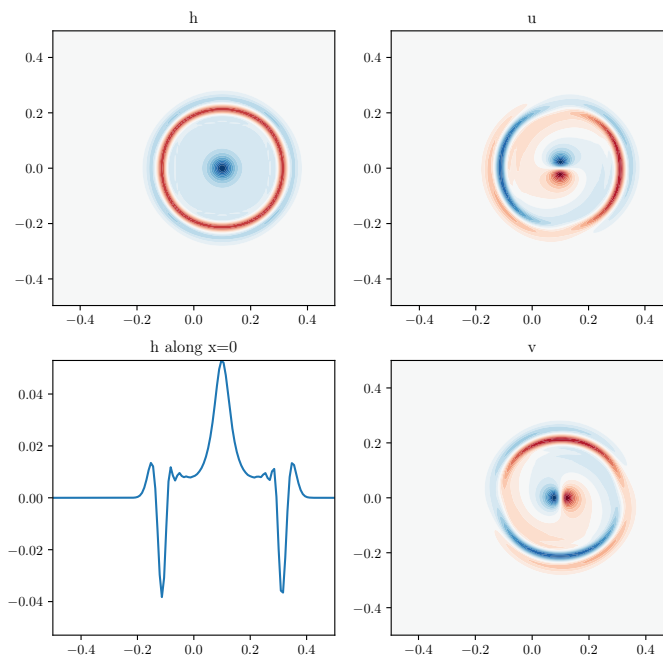
Figure 3.6: Coriolis term

Figure 3.6 indicates some initial disturbance, usually caused by the incoming water

waves by the basin tributaries. The generated gravity waves starts propagating away from the initial point. The inclusion of coriolis term usually important for assessing the effect of geostrophic implication, makes a significant effect on the turbulence. The results indicates that reflection of the waves is minimal. This is shown in Figure 3.7, whereby there is no reflection and the gravity wave is completely unstable. Flood waves therefore goes over bank and finally, there is little to contain the waves back into the basin, which causes havoc to the surrounding area.

The second snapshot of the shalllow water simulations indicates the results obtained after lengthy time evolution. A keen observation was made as captured in Figure 3.7. The wave disturbances shows results almost similar to common waves that could be classified as Coastal Kelvin as well as Rossby Waves that occurs in lakes or oceans[36]. The solution shows that the generated waves dissipates away from the disturbance with more energy. Since the boundary is assumed to be zero, such that $y = 0$ due to presence of dykes, the generated waves further decay exponentially away from the source.
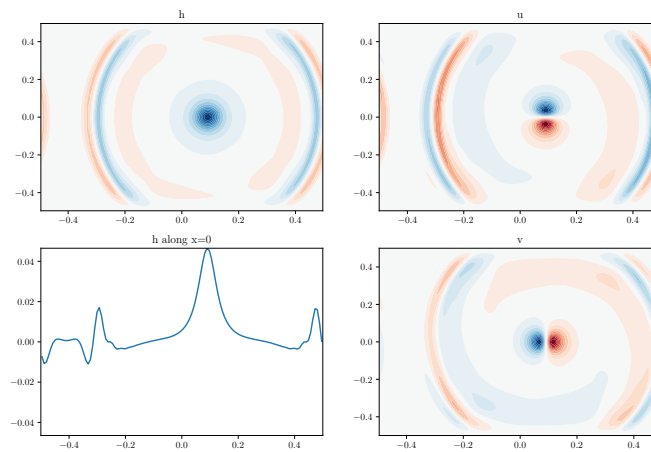
Figure 3.7: Wave Decay

As indicated in the previous Figure 3.6, this Figure 3.7 shows that as time evolves, the wave is tending to decay with different behaviours. To their opposite directions, the wave keeps decaying with indication of reflective behavour. However, as the number of days increases, it is clear that there is weak reflection. The motivating factor for the increase in the reflection is the addition of the sink term to the behavior of the model. This is what could have led to decrease in energy or increased reflections and therefore reduce the damage caused to the environment. This is the reason for the current study. Some of the proposed ways of introducing

sink is through consistent maintenance of the flood plain by continued emptying of the sediments such as sand or soil. These are activities that can employ economical ways, such as using the sand or the soil for other purposes. Alternatively, a dam may have a proper solution to this problem.

Chapter 4

Summary, Conclusions and Recommendations

4.1 Summary

The study sought to formulate a $2D$ flood wave model for Budalang'i flood plain, analyse the model and simulate the results with application to the Budalang'i flood plain domain. The development revealed that averaging of the $3D$ Navier Stokes equation yield an appropriate model for Budalang'i flood plain without many assumptions. From the analysis, it was found that the most likely waves occurring in the area were gravity waves. In addition, since the kinetic velocity (surface velocity) was greater than the potential velocity (phase speed) leading to a large Froude number, the flow was classified to be supercritical. This flow was therefore mainly due to gravitational force with strong influence of friction and Coriolis force as a result of closeness to the equatorial region. The findings further shows that there was formation of weakly reflecting waves. It can thus be concluded from the findings that adoption of measures such as digging of boreholes to improve the reflection back to the center of the waves would improve the reduction of the

47

energy within the flood plain.

4.2   Conclusions

The findings indicated that $3D$ Navier Stockes equation under assumption of averaging velocity fields and nearness to the equatorial region for the Budalang'i flood plain easily resulted to an appropriate $2D$ Shallow water model for Budalang'i flood plain. Addition of the sink term was appropriate for capturing the water variations due to infiltration, evaporation or boreholes through direct inclusion. In the analysis, it was concluded that Budalng'i flood plain experiences supercritical flows resulting from heavy rainfall during flooding. These are flows that lead to higher velocity of the propagating waves thus causing havoc in the surrounding regions. Finally, after successful simulations, the study concludes that the supercritical flows are responsible for turbulent flows and overbank flows but are easily controlled by addition of sink term such as a borehole.

4.3   Recommendations

From the findings, the study recommends a comprehensive formulation of a sink term to clearly capture flood attenuation in the $2D$ shallow water equations. In addition, further improvement should be made on the analysis of the $2D$ shallow water equations in order to enable explore a variety of physical areas including violent flows, rotating flows and other types of flows that could practically occur in any domain of flow. The study further recommends for improvement of the

current model to enable simulation of the complex topographies in other flood plain areas, which can increase reflection within the flood plains and reduce the energy due to the waves as well as the havoc caused in the surrounding region.

References

[1] Ambuchi J., *Flood Disaster Preparedness and Management in Schools: A Case Study of Budalangi Area in Busia County,*University of Nairobi, Kenya, (2011).

[2] Alcrudo F., *Mathematical Modelling Techniques for Flood Propagation in Urban Areas.* IMPACT Project Technical Report. 18, (2018),77.

[3] Alcrudo F and Pilar G., *A high-resolution Godunov-type scheme in finite volumes for the 2D shallow-water equations.* International Journal for Numerical Methods in Fluids **6**, (1993), 489-505.

[4] Alfred O., *Floods in Kenya*, In Developments in Earth Surface Processes, Elsevier **16**, (2013), 315-330.

[5] Altaie H., *New nested grids technique for 2D shallow water equations.* Diss. Universit Cte d'Azur, (2018).

[6] Bailey, Clare L. *Mathematical modelling of shallow water flows with application to Moreton Bay.* Brisbane. Diss. Loughborough University, (2010).

[7] Bashar K., Mutua F., Mulungu D., Deksyos T. and Shamseldin A., *Appraisal study to select suitable Rainfall-Runoff model for the Nile River Basin.* Proceedings of International Conference of UNESCO Nile Project,(2005), 1215.

[8] Bates P., Lane S., and Ferguson R., *Computational Fluid Dynamics: Applications in Environmental Hydraulics*, John Wiley and Sons, 2005.

REFERENCES

[9] Bernadelli H., *Water Waves*, Journal of the Burma Research Society **31** (2003), 1-18.

[10] Bernadelli H., *Mathematical modeling techniques for flood propagation in urban areas*, Journal of the Burma Research Society **25**, (2013), 1-4.

[11] Bloch I., Jean D. and Sylvain N., *Quantum simulations with ultracold quantum gases.* Nature Physics **8**, (2012), 267-276.

[12] Boroughs C. and Edie Z., *Daily flow routing with the Muskingum-Cunge method in the Pecos River RiverWare model*, Proceedings of the Second Federal Interagency Hydrologic Modeling Conference, Las Vegas, NV, July. 2002.

[13] Carol A., and Lakshmi H., *Numerical Models of Oceans and Oceanic Processes,* Elsevier, 2000.

[14] Drought Monitoring Centre-Nairobi., *Coping with Floods in Kenya: Vulnerability, Impacts and Adaptation Options for the Flood Prone Areas of Western Kenya,* DMCN-UNEP project report, 2004.

[15] Delis A. and Katsaounis T., *Numerical solution of the two-dimensional shallow water equations by the application of relaxation methods*, Applied Mathematical Modelling, **8**, (2005) 754-783.

[16] Eitel B., and Ochola, S., (2006). River Nyando Basin Project (Institute of Geography, University of Heidelberg). Available at http://www.geog.uni-heidelberg.de/physio/forschung/nyandobasin.htm

[17] Elena M., *The shallow water model: The relevance of geometry and turbulence*, Monographs of the Royal Academy of Sciences of Zaragoza **31**, (2009), 217-236.

REFERENCES

[18] Ersoy M.,, *Shallow water equations: Modeling, numerics and applications.*, University of Sussex, (2013).

[19] Ferrari S. and Fausto S., *A new two-dimensional Shallow Water model including pressure effects and slow varying bottom topography.* ESAIM: Mathematical Modelling and Numerical Analysis **38**, (2004), 211-234.

[20] Fredrick M., *Integration of remote sensing (RS) and Geographic information system (GIS) in Monitoring and management of floods*, Masters Project, Nairobi University, (2011)

[21] Jain S. and Sharad K., *A Brief review of flood forecasting techniques and their applications.* International Journal of River Basin Management **16.3** (2018), 329-344.

[22] Hamrick A., *Analysis of the numerical solution of the shallow water equations.* Naval Postgraduate School Monterey, (1997), 18-29.

[23] Hervouet J., *A high resolution 2D dam-break model using parallelization.* Laboratoire National Hydraulique-EDF-DER. Hydrological Processes **6**, (2000),2211-2230.

[24] Hirt C. and Nichols F., *Volume of fluid (VOF) method for the dynamics of free boundaries*, Journal of computational physics **39**, (1981), 201-225.

[25] Jasem M. and Ismail I., *Approximate Methods for the Estimation on of Muskingum Flood.* Journal of Water Resources Management Publisher Springer Netherlands **20**, (2006), 1573-1650.

[26] Kivula V., Otengi S. and Miima J., *Rainfall Runoff Modelling in River Yala Basin, Western Kenya Kenya*, Journal of Science Technology Education and Management **20**, (2018), 21-28.

REFERENCES

[27] Kiluva V., Mutua F., Makhanu S. and Ongor B., *Application of the geological streamflow and muskingum cunge models in the Yala River Basin-Kenya.* Journal of Agriculture, Science and Technology **2**, (2011),13-14.

[28] Kizza M., Allan R. and Henry K., *Modelling catchment inflows into Lake Victoria, uncertainties in rainfallrunoff modelling for the Nzoia River* Hydrological Sciences Journal **56**, (2011), 1210-1226.

[29] Lakshmi H. Kantha and Carol Anne Clayson. Numerical Models of Oceans and Oceanic Processe. Acadmic Press, **2**,(2000)

[30] Landau L. and Akhiezer I., *General physics: mechanics and molecular physics*, Pergamon London **12**, (2013), 4-5.

[31] Leveque R. and Randall J., *Finite volume methods for hyperbolic problems* Vol. 31. Cambridge university press, 2002.

[32] Macchione F., *Application of the Muskingum-Cunge method for dam break flood routing.* WIT Transactions on Ecology and the Environment **8**, (1970), 14-17.

[33] Marche F., *Derivation of a new two-dimensional viscous shallow water model with varying topography, bottom friction and capillary effects*, European Journal of Mechanics-B/Fluids **26**, (2007), 49-63.

[34] MWRMD, Ministry of Water Resources Management and Development-Strategy for Flood Management for Lake Victoria Basin, Kenya.

[35] Muis S., Burak G., Brenden J. and Philip J., *Flood risk and adaptation strategies under climate change and urban expansion: A probabilistic analysis using global data.* Science of the Total Environment **538**, (2015), 445-457.

REFERENCES

[36] Murillo J., and Garca P., *Weak solutions for partial differential equations with source terms. Application to the shallow water equations.* Journal of Computational Physics **229**, (2010), 4327-4368.

[37] Mutua F. and Willy B., *Climate change impact on SWAT simulated streamflow in western Kenya."* International Journal of Climatology, A Journal of the Royal Meteorological Society **29**,(2009), 1823-1834.

[38] Mutua F., Mtalo F. and Bauwens W., *Challenges of Modeling the Flows of the Nile River.* Proceedings of International Conference of UNESCO Flanders Fust Friend/Nile Project Towards A Better Cooperation And The 5th Project Management Meeting And 9th Steering Committee Meeting (2005) Nov (pp. 12-15).

[39] Nath K. and Sen D., *Finite Volume Model for Shallow Water Equations with Improved Treatment of Source Terms.*Journal of Hydraulic Engineering **134**, (2008), 626-635.

[40] Ponce M., and Simons B., *Shallow wave propagation in open channel.* Journal of Hydraulic Engineering **198**, (1977), 747758.

[41] Shrestha R. and Franz N., *River Water Level Prediction Using Physically Based and Data Driven Models.* Journal of Hydrology **11**, (2019), 15-81.

[42] Tewolde M., Mesfin H. and Smithers J., *Flood routing in ungauged catchments using Muskingum methods.* Water SA **32**,(2006), 379-388.

[43] Welch J., *Integrating a Bilinear Interpolation Function Across Quadrilateral Cell Boundaries*, Technical Report No. LA-UR-00-3329. Los Alamos National Lab., NM (US),(2001)

REFERENCES

[44] Townsend A.,and Philip J., Numerical simulation of the shallow water equations coupled with a precipitation system driven by random forcing. Diss. University of Sussex, (2018).

[45] Zoppou P., *Second-order approximate Riemann solver with a van Leer type limiter* ,Biometrika **33**, (2007), 183-212.

Appendices

Appendix A

Shallow Water Code

```
import time
import numpy as np
import matplotlib.pyplot as plt
import viz-tools
```

$prameters - - - - - - - - - - - - - - -$

$L_x = 1E + 4$ Length of domain x-direction in meters

$L_y = 1E + 4$ Length of domain y-direction in meters

$g = 9.81$ Acceleration of gravity $[m/s^2]$

$H = 1.5$ Maximum depth of fluid $[m]$

$f_0 = 1E - 5$ Fixed part of coriolis parameter $[1/s]$

$\beta = 2E - 11$ gradient of coriolis parameter $[1/ms]$

$use - coriolis = True$ True if you want coriolis force

$use - friction = False$ True if you want bottom friction

$use - wind = False$ True if you want wind stress

$use - source = False$ True if you want mass source into the domain

$use - sink = False$ True if you want mass sink out of the domain

$param - string = " \backslash n =$

"

$param_string+ = "\nuse-friction = {}\nuse-wind = {}".format(use-friction, use-wind)$

$param_string+ = "\nuse-source = {}\nuse-sink = {}".format(use-source, use-sink)$

$param_string+ = "\ng = {: g}\nH = {: g}".format(g, H)$

———————— Computational prameters ————————

$N_x = 150$ Number of grid points in x-direction

$N_y = 150$ Number of grid points in y-direction

$dx = L_x/(N_x - 1)$ Grid spacing in x-direction

$dy = L_y/(N_y - 1)$ Grid spacing in y-direction

$dt = 0.1 * min(dx, dy)/np.sqrt(g * H)$ Time step (defined from the CFL condition)

$time-step = 1$ For counting time loop steps

$max-time_step = 5000$ Total number of time steps in simulation

$x = np.linspace(-L_x/2, L_x/2, N_x)$ Array with x-points

$y = np.linspace(-L_y/2, L_y/2, N_y)$ Array with y-points

$X, Y = np.meshgrid(x, y)$ Meshgrid for plotting

$X = np.transpose(X)$ To get plots right

$Y = np.transpose(Y)$ To get plots right

$param-string+ = "\ngndx = : .2fkm\ndy = : .2fkm\ndt = : .2fs".format(dx, dy, dt)$

Define friction array if friction is enabled

$if(use-frictionisTrue) :$

$kappa_0 = 1/(5 * 24 * 3600)$

$kappa = np.ones((N_x, N_y)) * kappa_0$

$kappa[0, :] = kappa_0$

$kappa[-1,:] = kappa_0$

$kappa[:,0] = kappa_0$

$kappa[:,-1] = kappa_0$

$kappa[:int(N_x/15),:] = 0$

$kappa[int(14*N_x/15)+1:,:] = 0$

$kappa[:,:int(N_y/15)] = 0$

$kappa[:,int(14*N_y/15)+1:] = 0$

$kappa[int(N_x/15):int(2*N_x/15),int(N_y/15):int(14*N_y/15)+1] = 0$

$kappa[int(N_x/15):int(14*N_x/15)+1,int(N_y/15):int(2*N_y/15)] = 0$

$kappa[int(13*N_x/15)+1:int(14*N_x/15)+1,int(N_y/15):int(14*N_y/15)+1] = 0$

$kappa[int(N_x/15):int(14*N_x/15)+1,int(13*N_y/15)+1:int(14*N_y/15)+1] = 0$

$param_string+ = "\nkappa =: g\nkappa/beta =: gkm".format(kappa_0, kappa_0/(beta*1000))$

Define wind stress arrays if wind is enabled. $if(use_windisTrue):$

$tau_x = -tau_0 * np.cos(np.pi * y/L_y) * 0$

$tau_y = np.zeros((1, len(x)))$

$param_string+ = "\ntau_0 =: g\nrho_0 =: gkm".format(tau_0, rho_0)$

$Definecoriolisarrayifcoriolisisenabled.$

$if(use_coriolisisTrue):$

$if(use_betaisTrue):$

$f = f_0 + beta * y$ $Varyingcoriolisparameter$

$L_R = np.sqrt(g * H)/f_0$

$c_R = beta * g * H/f_0 ** 2$

$else:$

$f = f_0 * np.ones(len(y))$ $Constantcoriolisparameter$

$alpha = dt * f$ $Parameterneededforcoriolisscheme$

$beta_c = alpha ** 2/4$ $Parameter needed for coriolis scheme$

$param_string+ = "\nf_0 =: g".format(f_0)$

$param_string+ = "\nMax alpha =: g\n".format(alpha.max())$

$param_string+ = "\nRossby radius ::.1fkm".format(L_R/1000)$

$param_string+ = "\nRossby number :: g".format(np.sqrt(g * H)/(f_0 * L_x))$

$param_string+ = "\nLong Rossby wave speed ::.3fm/s".format(c_R)$

$param_string+ = "\nLong Rossby transit time ::.2fdays".format(L_x/(c_R * 24 * 3600))$

$param_string+ = "\n ===$

$\n"$ Define source array if source is enabled.

$if(use_source):$

$sigma = np.zeros((N_x, N_y))$

$sigma = 0.0001 * np.exp(-((X - L_x/2) ** 2/(2 * (1E + 5) ** 2) + (Y - L_y/2) ** 2/(2 * (1E + 5) ** 2)))$ Define source array if source is enabled.

$if(use_sink is True):$

$w = np.ones((N_x, N_y)) * sigma.sum()/(N_x * N_y)$ Write all parameters out to file.

$with open("param_output.txt", "w") as output_file:$

$output_file.write(param_string)$

$print(param - string) Also print parameters to screen$

$==================== Allocating arrays and initial conditions ==========$

$u_n = np.zeros((N_x, N_y))$ To hold u at current time step

$u_np1 = np.zeros((N_x, N_y))$ To hold u at next time step

$v_n = np.zeros((N_x, N_y))$ To hold v at current time step

$v_np1 = np.zeros((N_x, N_y))$ To hold v at enxt time step

$eta_n = np.zeros((N_x, N_y))$ To hold eta at current time step

$eta_np1 = np.zeros((N_x, N_y))$ To hold eta at next time step

Temporary variables (each time step) $h_e = np.zeros((N_x, N_y))$

$h_w = np.zeros((N_x, N_y))$

$h_n = np.zeros((N_x, N_y))$

$h_s = np.zeros((N_x, N_y))$

$uhwe = np.zeros((N_x, N_y))$

$vhns = np.zeros((N_x, N_y))$

Initial conditions for u and v. $u_n[:,:] = 0.0$ Initial condition for u

$v_n[:,:] = 0.0$ Initial condition for u

$u_n[-1,:] = 0.0$ Ensuring initial u satisfy BC

$v_n[:,-1] = 0.0$ Ensuring initial v satisfy BC

     Initial condition for eta.

$eta_n[:,:] = np.sin(4 * np.pi * X/L_y) + np.sin(4 * np.pi * Y/L_y)$

$eta_n = np.exp(-((X - 0) ** 2/(2 * (L_R) ** 2) + (Y - 0) ** 2/(2 * (L_R) ** 2)))$

$eta_n = np.exp(-((X - L_x/2.7) ** 2/(2 * (0.05E + 6) ** 2) + (Y - L_y/4) ** 2/(2 *$
$(0.05E + 6) ** 2)))$

$eta_n[int(3 * N_x/8) : int(5 * N_x/8), int(3 * N_y/8) : int(5 * N_y/8)] = 1.0$

$eta_n[int(6 * N_x/8) : int(7 * N_x/8), int(6 * N_y/8) : int(7 * N_y/8)] = 1.0$

$eta_n[int(3 * N_x/8) : int(5 * N_x/8), int(13 * N_y/14) :] = 1.0$

$eta_n[:,:] = 0.0$

$viz_tools.surface-plot2D(X, Y, eta_n, (X.min(), X.max()), (Y.min(), Y.max()), (eta_n.min(), etc$

Sampling variables.

$eta_list = list(); u_list = list(); v_list = list()$ Lists to contain eta and u,v
for simulation

=============== $Done with setting up arrays and initial conditions$ ==========

$t_0 = time.perf - counter()$ For timing the computation loop

$======================= Maintimeloopforsimulation =========$

$===$

$while(time_step < max_time_step):$

$----------- Computing values for u and v at next time step -----$

$----------$

$u_np1[:-1,:] = u_n[:-1,:] - g*dt/dx*(eta_n[1:,:] - eta_n[:-1,:])$

$v_np1[:,:-1] = v_n[:,:-1] - g*dt/dy*(eta_n[:,1:] - eta_n[:,:-1])$

$Add friction if enabled.$

$if(use_friction is True):$

$u_np1[:-1,:]-= dt*kappa[:-1,:]*u_n[:-1,:]$

$v_np1[:-1,:]-= dt*kappa[:-1,:]*v_n[:-1,:]$

Add wind stress if enabled.

$if(use_wind is True):$

$u_np1[:-1,:]+= dt*tau_x[:]/(rho_0*H)$

$v_np1[:-1,:]+= dt*tau_y[:]/(rho_0*H)$

Use a corrector method to add coriolis if it's enabled.

$if(use_coriolis is True):$

$u_np1[:,:] = (u_np1[:,:] - beta_c*u_n[:,:] + alpha*v_n[:,:])/(1+beta_c)$

$v_np1[:,:] = (v_np1[:,:] - beta_c*v_n[:,:] - alpha*u_n[:,:])/(1+beta_c)$

$v_np1[:,-1] = 0.0$

upper boundary condition

$u_np1[-1,:] = 0.0$

left boundary condition

$------------------------- Done with u and v -----$

$------------------------------ h_e[:-1,:] = np.where(u_np1[:$

$-1,:] > 0, eta_n[:-1,:] + H, eta_n[1:,:] + H)$

$h_e[-1,:] = eta_n[-1,:] + H$

$h_w[0,:] = eta_n[0,:] + H$

$h_w[1:,:] = np.where(u_np1[:-1,:] > 0, eta_n[:-1,:] + H, eta_n[1:,:] + H)$

$h_n[:,:-1] = np.where(v_np1[:,:-1] > 0, eta_n[:,:-1] + H, eta_n[:,1:] + H)$

$h_n[:,-1] = eta_n[:,-1] + H$

$h_s[:,0] = eta_n[:,0] + H$

$h_s[:,1:] = np.where(v_np1[:,:-1] > 0, eta_n[:,:-1] + H, eta_n[:,1:] + H)$

$uhwe[0,:] = u_np1[0,:] * h_e[0,:]$

$uhwe[1:,:] = u_np1[1:,:] * h_e[1:,:] - u_np1[:-1,:] * h_w[1:,:]$

$vhns[:,0] = v_np1[:,0] * h_n[:,0]$

$vhns[:,1:] = v_np1[:,1:] * h_n[:,1:] - v_np1[:,:-1] * h_s[:,1:]$

——————————————- first computations done ———————————-

$-------------------Computing \eta values at next timestep ---$

$----------------------$

$\eta_np1[:,:] = \eta_n[:,:] - dt * (uhwe[:,:]/dx + vhns[:,:]/dy)$

Add source term if enabled. $if(use_source is True):$

$eta_np1[:,:] += dt * sigma$

Add sink term if enabled. $if(use_sink is True):$

$eta_np1[:,:] -= dt * w$

$--Done with eta -$

$--$

$u_n = np.copy(u_np1)$ Update u for next iteration $v_n = np.copy(v_np1)$ Update v for next iteration

$eta_n = np.copy(eta_np1)$ Update eta for next iteration

$time_step += 1$

$if(time_step sample_interval == 0):$

$hm_sample.append(eta_n[:, int(N_y/2)])$

$ts_sample.append(eta_n[int(N_x/2), int(N_y/2)])$

$t_sample.append(time_step * dt)$

Store eta and (u, v) every anin-interval time step for simulations.

$if(time_stepprint("Time : \t: .2fhours".format(time_step * dt/3600))$

$print("Step : \t/".format(time_step, max_time_step))$

$print("Mass : \t\n".format(np.sum(eta_n)))$

$u_list.append(u_n)$

$v_list.append(v_n)$

$eta_list.append(eta_n) ============================= Maintimeloopdone$

$print("Maincomputationloopdone!\nExecutiontime : : .2fs".format(time.perf_counter() -$

$t_0)) print("\nVisualizingresults...") ================= Visualizingresults ==$

$viz_tools.pmesh_plot(X, Y, \eta_n, \Finalstateofsurfaceelevation\eta")$

$viz_tools.quiver_plot(X, Y, u_n, v_n, "Finalstateofvelocityfield\mathbf{u}(x, y)")$

$viz_tools.hovmuller_plot(x, t_sample, hm_sample)$

$viz_tools.plot_time_series_and_f t(t_sample, ts_sample)$

$eta_anim = viz_tools.eta_animation(X, Y, \eta_list, anim_interval * dt, "\eta")$

$eta_surf_anim = viz_tools.eta_animation3D(X, Y, \eta_list, anim_interval*dt, "\eta_surface")$

$quiv_anim = viz_tools.velocity_animation(X, Y, u_list, v_list, anim_interval*dt, "velocity")$

$print("\Visualizationdone!")$

$plt.show()$